FOR FURTHER TRAN *TL TW*

RADC-TR-78-80
Final Technical Report
April 1978

REAL TIME ATMOSPHERIC MONITOR

Itek Corporation

Sponsored by
Defense Advanced Research Projects Agency (DoD)
ARPA Order No. 2646

Approved for public release; distribution unlimited.

The views and conclusions contained in this document are those
of the authors and should not be interpreted as necessarily
representing the official policies, either expressed or implied,
of the Defense Advanced Research Projects Agency or the U.S.
Government.

ROME AIR DEVELOPMENT CENTER
Air Force Systems Command
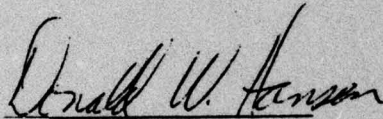Griffiss Air Force Base, New York 13441

DDC
RECEIVED
MAY 24 1978
A

This report has been reviewed by the RADC Information Office (OI) and is releasable to the National Technical Information Service (NTIS). At NTIS it will be releasable to the general public, including foreign nations.

RADC-TR-78-80 has been reviewed and is approved for publication.

APPROVED: *Donald W. Hanson*

DONALD W. HANSON
Project Engineer

REAL TIME ATMOSPHERIC MONITOR

Alan J. MacGovern

Contractor: Itek Corporation
Contract Number: F30602-74-C-0147
Effective Date of Contract: 18 March 1974
Contract Expiration Date: 20 July 1976
Short Title of Work: Real Time Atmospheric Monitor
Program Code Number: 6E20
Period of Work Covered: March 1974 - January 1977

Principal Investigator: A. J. MacGovern
                Phone: (617) 276-3075

Project Engineer: Donald W. Hanson
              Phone: (315) 330-3144
                      Autovon 587-3144

Approved for public release; distribution unlimited.

SECURITY CLASSIFICATION OF THIS PAGE *(When Data Entered)*

REPORT DOCUMENTATION PAGE	READ INSTRUCTIONS BEFORE COMPLETING FORM

1. REPORT NUMBER	2. GOVT ACCESSION NO.	3. RECIPIENT'S CATALOG NUMBER
RADC-TR-78-80		

4. TITLE (and Subtitle)

REAL TIME ATMOSPHERIC MONITOR,

5. TYPE OF REPORT & PERIOD COVERED

Final Technical Report.
Mar 74 - Jan 77.

6. PERFORMING ORG. REPORT NUMBER

PFR-78-006

7. AUTHOR(s)

Alan J. MacGovern

8. CONTRACT OR GRANT NUMBER(s)

F30602-74-C-0147,
ARPA Order-2646

9. PERFORMING ORGANIZATION NAME AND ADDRESS

Itek Corporation
10 Maguire Road
Lexington MA 02173

10. PROGRAM ELEMENT, PROJECT, TASK AREA & WORK UNIT NUMBERS

62301E
26460104 01

11. CONTROLLING OFFICE NAME AND ADDRESS

Defense Advanced Research Projects Agency
1400 Wilson Boulevard
Arlington VA 22209

12. REPORT DATE

Apr 1978

13. NUMBER OF PAGES

39 38 p.

14. MONITORING AGENCY NAME & ADDRESS(if different from Controlling Office)

Rome Air Development Center (OCSE)
Griffiss AFB NY 13441

15. SECURITY CLASS. (of this report)

UNCLASSIFIED

15a. DECLASSIFICATION/DOWNGRADING SCHEDULE

N/A

16. DISTRIBUTION STATEMENT (of this Report)

Approved for public release; distribution unlimited.

17. DISTRIBUTION STATEMENT (of the abstract entered in Block 20, if different from Report)

Same

18. SUPPLEMENTARY NOTES

RADC Project Engineer:
Donald W. Hanson (OCSE)

19. KEY WORDS (Continue on reverse side if necessary and identify by block number)

Optical transfer function
Atmospheric turbulence
Telescope imaging
Diffraction gratings

20. ABSTRACT (Continue on reverse side if necessary and identify by block number)

This report discusses the Real Time Atmospheric Measurement (RTAM) system constructed for the purpose of obtaining short-exposure optical transfer function (OTF) measurements of the atmosphere/telescope combination for the 1.6-meter telescope at the AMOS Observatory on Maui, Hawaii. A description of the principle of operation of the RTAM is given together with a parametric analysis detailing the operating characteristics and expected signal-to-noise ratios. The instrument uses star light focused onto rotating diffraction

DD FORM 1473 EDITION OF 1 NOV 65 IS OBSOLETE
1 JAN 73

SECURITY CLASSIFICATION OF THIS PAGE *(When Data Entered)*

404 157

gratings to make the OTF measurements. The characteristics of these gratings are described, together with the electro-optical and electromechanical details of the system.

The RTAM underwent initial installation tests in August 1966. As a result of those tests, certain electrical and optical modifications were designed and implemented. The details of these modifications are given. The modified equipment was reinstalled in January 1977. The equipment was found to have an acceptable field of view, and for single-channel operation, gave signal-to-noise ratio results close to those predicted by the parametric analysis.

CONTENTS

iii

FIGURES

1. INTRODUCTION

ABSTRACT

The most widely accepted measure of the performance of any imaging optical system is the optical transfer function (OTF). The OTF is made up of two functions namely, the modulation transfer function (MTF) and the phase transfer function (PTF), which are simply defined as the modulation and phase of the image of an sinusoidal input object, measured as a function of the spatial frequency of the sinusoid. Ground-based telescopes provide images that are deteriorated by atmospheric turbulence, and the OTF used to describe the performance of the total imaging system must take into account the effects of the atmosphere. The Real Time Atmospheric Measurement (RTAM) system was designed to measure the telescope/atmosphere OTF for the 1.6-meter telescope at the ARPA Maui Optical Station (AMOS) atop Haleakala volcano on the island of Maui, Hawaii. Specifically the instrument was designed to provide multiple short-exposure (10^{-3} second) (.001 second) samples of the system OTF using light from bright stars for making the measurement.

This report describes the RTAM instrument developed by Itek Corporation, together with test results. ABSTRACT

2. TECHNICAL APPROACH

2.1 SYSTEM SPECIFICATIONS

The principal specifications to be met by the RTAM system were as follows:

1. Provide orthogonal samples of the two-dimensional optical transfer function (OTF) (both modulus and phase) every 8 milliseconds, with exposure times of $\leq 10^{-3}$ second.

2. Provide means for orienting the orthogonal OTF slices at any angle

3. Operate over a wavelength band of 0.4 to 0.7 micrometer.

4. Provide a signal-to-noise ratio at the DC of the modulation transfer function (MTF) of $>33:1$ for a first magnitude star and greater than $3:1$ for a fifth magnitude star.

2.2 LATERAL SHEARING INTERFEROMETER

The system designed to provide the OTF information according to the specifications was a variable lateral shear white light interferometer, it comprised two sets of rotating gratings suitably imaged on one another so as to give the optical equivalent of two identical linear gratings lying in the same plane and rotating in opposite directions. The star image formed by the telescope (and modified by the atmosphere) is focused in this grating pair at a point some distance from the common rotation axis. At the moment the grating lines on one grating are exactly parallel to those on the other, the cone of rays formed by the 0, +1 transmission order (0 being zero-order through the first grating, and +1 being one first-order diffracted beam from the second) exactly overlap the −1, 0 order, interference will take place over the complete pupil. When the gratings rotate so the grating line directions make an angle, the overlap of the transmitted 0, +1 and −1, 0 cones is only partial. Effectively then, two images of the telescope are sheared with respect to each other by rotation of the gratings. Fig. 2-1 illustrates the geometry of the sheared images. Because the focused cone is at a point distant from the rotation axis of the two gratings, the motion of one with respect to the other consists of both rotation and translation. The rotation component imparts the variable shear and the translation imposes a positive Doppler shift to one diffracted order and a negative Doppler shift to the other, so that where they overlap they interfere with a beat frequency of $2\pi\omega$, where $2\pi\omega/2$ is the frequency that the grating lines pass the focus point. This is independent of wavelength so that the system operates in white light.

Let the wavefront in the telescope pupil be represented by A(x, y) where

$$A(x, y) = a(x, y) \exp\left[ikW(x, y)\right]$$

where W(x, y) is the wave aberration, and $k = 2\pi/\lambda$, where λ is the wavelength of the light.

0, 1 ⎫ Diffracted
1, 0 ⎭ cones

Grating lines

Overlap region

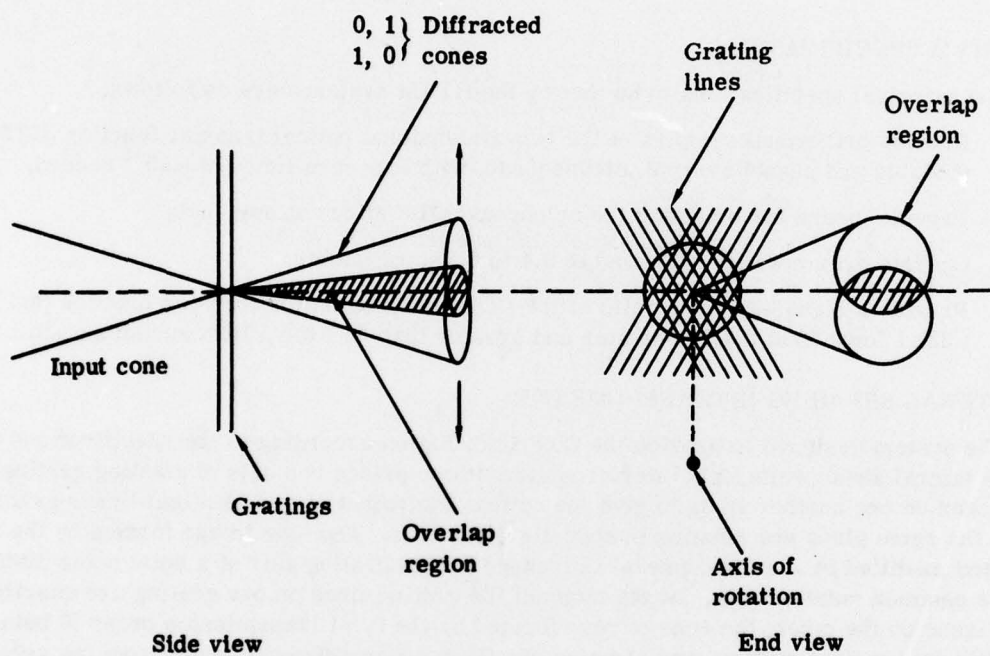Input cone

Gratings

Overlap region

Axis of rotation

Side view

End view

Fig. 2-1 — Cones diffracted by rotating gratings

The total flux $F(\Delta x)$ in the sheared interference pattern is given by

$$F(\Delta x) = \iint \left| A\left(x - \frac{\Delta x}{2}, y\right) + A\left(x + \frac{\Delta x}{2}, y\right) \exp(iwt) \right|^2 dx\, dy$$

$$= 2 \iint |A(x, y)|^2 dx\, dy + \left[\exp(-iwt) \iint A\left(x - \frac{\Delta x}{2}, y\right) \right.$$

$$\left. A^*\left(x + \frac{\Delta x}{2}, y\right) dx\, dy \right] + [\quad]^*$$

The function

$$\frac{\iint A(x + \Delta x, y)\, A^*(x - \Delta x, y)\, dx\, dy}{|A(x, y)|^2 dx\, y} = T(\Delta x) \cdot \exp[i\phi(\Delta x)]$$

is by definition the optical transfer function (being the autocorrelation of the pupil function) where $T(\Delta x)$ is the MTF and $\phi(\Delta x)$ is the phase transfer function (PTF), thus

$$F(\Delta x) = 2c\{1 + T(\Delta x) \cos[wt - \phi(\Delta x)]\}$$

where $c = \iint |A(x, y)|^2 dx\, dy$ and represents the total optical flux in the two beams.

Thus the output of a detector placed to intercept the interfering beams is an amplitude modulated cosine function whose modulation is the MTF of the system and whose phase is the PTF. Envelope detection on the detector output therefore gives the MTF and phase detection the PTF.

2.3 OPTICAL ARRANGEMENT

The original optical layout of the RTAM is shown in Fig. 2-2. Light from the prime telescope focus is collimated by lens L1 (a lens of variable position for fine control of instrument focus). The collimated light passes through a Dove prism (in a motorized rotating mount for pupil image rotation) and is refocused by lens L2 and a fold mirror onto the first grating G1. The light transmitted by the first grating is refocused onto the second grating by two microscope objectives (L3 and L4) and a K mirror set. Light transmitted by the second grating is transferred by fold mirrors and focusing lenses to two photodetectors, one for x shear and one for Y shear. (The orthogonal shears are formed by the grating structure as discussed below.) The two gratings are attached to a common rotating shaft. The K mirrors between the focus images gives the optical effect of having the two gratings in the same plane but rotating in opposite directions. The zero-order beam transmitted by the first grating is refocused onto the second grating where it is diffracted into orders of which the zero- and first-orders are dominant. The order of interest is the first-order from the second grating (denoted as the 0, 1 order), which interferes on the photodetector surface with the 1, 0 order (i.e., with the beam resulting from the first-order diffraction by the first grating, followed by zero-order transmissions through the second grating). These orders travel in basically the same direction to the photomultiplier photocathode(s) with all other orders being suitably baffled. As shown above, the envelope of the photomultiplier gives the MTF and the phase the PTF of the atmosphere/telescope combination when an unresolved star is focused by the telescope.
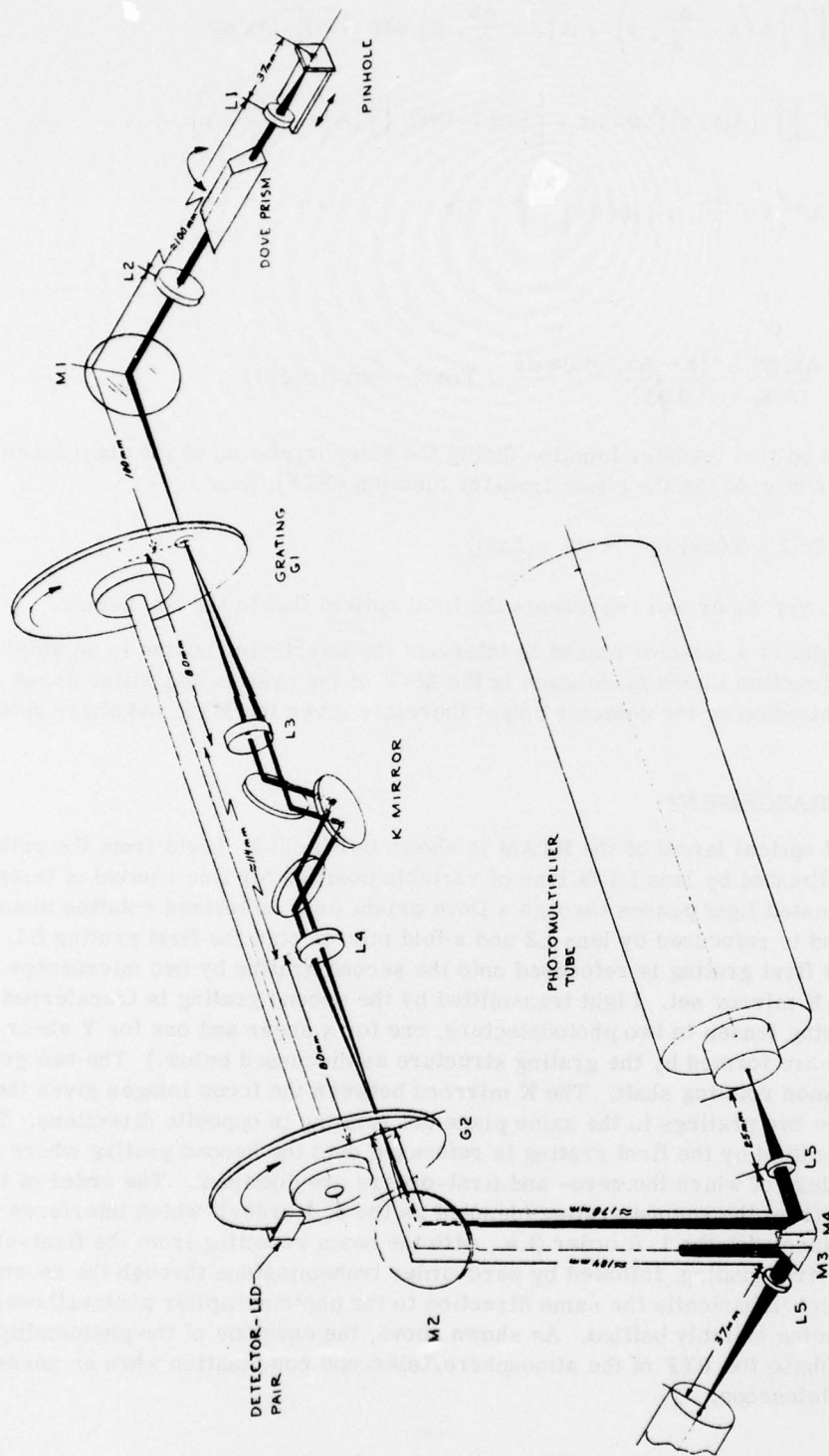
Fig. 2-2 — Original optical layout of RTAM

Gratings

Fig. 2-3 shows the grating structure used to provide the required MTF slices in two orthogonal directions, and to provide the required output time and repetition rates. Each grating disk consisted of eight grating sections alternately oriented so as to provide diffraction in two orthogonal directions. Grating sections 1, 3, 5, and 7 give slices in the X(say) direction through the two-dimensional MTF, and sections 2, 4, 6, and 8 give slices in the Y direction. The rotation period of the grating disks was 32 milliseconds so that an MTF slice (alternately X and Y) is produced every 4 milliseconds. Fig. 2-4 shows a timing diagram of the expected outputs.

The gratings used were 100-line-pair-per-millimeter blazed transmission gratings generated by an epoxy replication process by Bausch & Lomb. They were blazed so as to give equal zero- and first-order transmissions of 34 percent at 4200 Å, and to have especially uniform (< 3 percent variation) transmission properties with an f/64 focused beam. The interfering beams results from the transmission of the 0, 1 and 1, 0 orders and therefore the product of the zero- and first-order efficiencies is the important parameter. This product was measured to be ~0.1 and was essentially independent of wavelength.

To measure the noise on an f/64 beam transmitted through the gratings (either zero- or first-order) a telecentric scanning system using an oscillating mirror, a focused HeNe laser, and a photomultiplier was set up. Fig. 2-5 shows the resulting transmissions of sections of the accepted gratings.

2.4 ELECTRONIC SYSTEM

The electronic system was designed to provide as signal outputs on separate coaxial cables the X and Y slices of the MTF and the PTF. In addition, outputs of timing pulses (derived from fiducial marks on the edges of the grating disks) and other system functional values such as image rotation position and image focus, were required. The details of the original electronics has been described, together with circuit diagrams operating and maintenance instructions, in an earlier report.* Changes made to the electronics are described later in this report. The basic electronic processing performed to provide a particular channel (X or Y) MTF and PTF is illustrated in Fig. 2-6. The output of the photomultiplier (with an S20 photocathode) is transmitted via a video amplifier to a bandpass filter that is centered at the carrier frequency of approximately 370 kHz (governed by the line period and rotation rate of the gratings and position of the focused spots on the gratings). The output of the bandpass filter is transmitted to the MTF and PTF processing electronics. The MTF is formed by full-wave rectification of the ac signal followed by low pass filtering of variable bandwidth to act as envelope detection. The PTF circuitry originally included a phase locked loop, the low pass filtered output of which was integrated to give the change of phase with time. This system had limitations for low signal-to-noise ratio signals and was later modified to consist of a direct $\pm\pi$ phase measuring circuit using the output of a voltage controlled oscillator as a reference. This circuit is described in more detail later in this Report.

## 2.5 SYSTEM ANALYSIS

2.5.1 Parametric Analysis

2.5.1.1 Timing

The length of time occupied by each OTF output is a function of grating rotation period T, grating line spacing s, input beam cone angle α, and optical wavelength λ. Fig. 2-7 illustrates

---

*Itek Corporation, Real-Time Atmosphere Measurement System, Itek 75-9505-1, Operation and Maintenance Manual, July 1975.

Blaze
direction

X grating

Pilot
hole
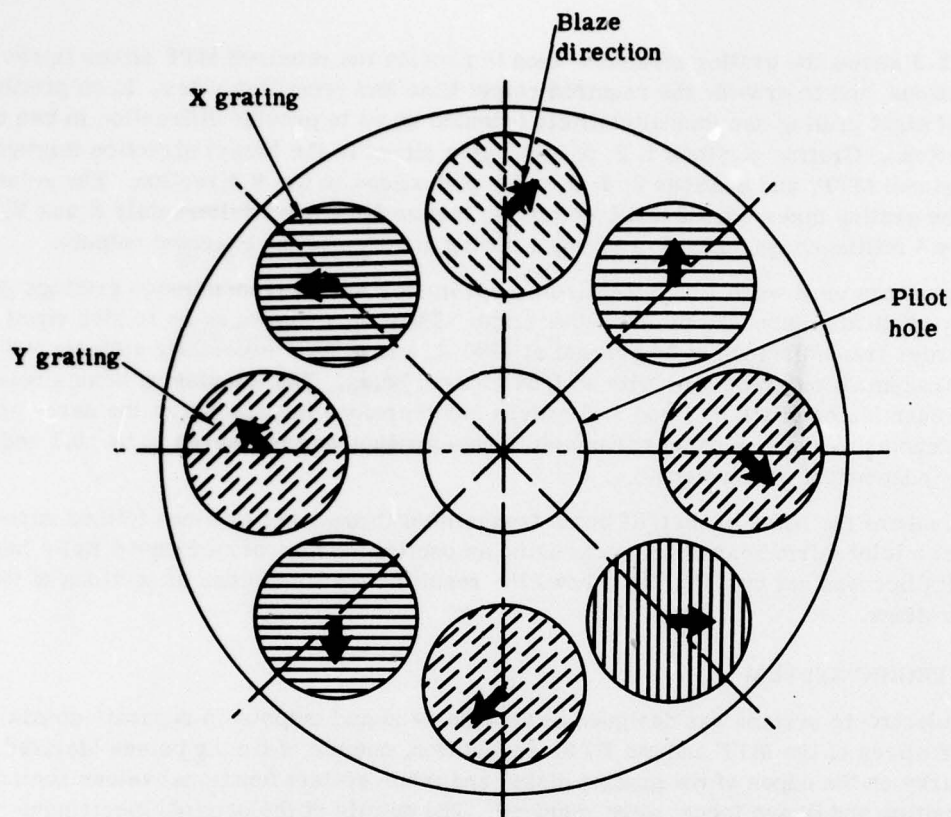
Y grating

Note: Eight gratings equally spaced. Grating lines lie at
45 degrees ± 15 arc-minutes to a radius from the
center of the pilot hole taken every 45 degrees.

Fig. 2-3 — Grating disks with eight grating sections

X   Y   X   Y   X

0   4   8   12   16

Time, milliseconds

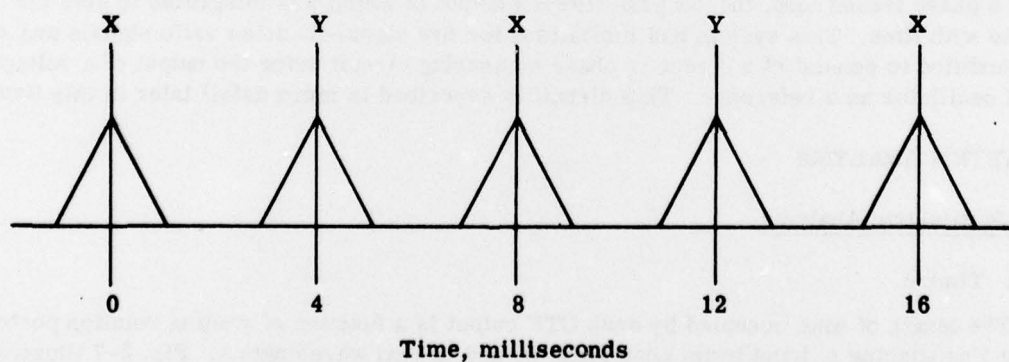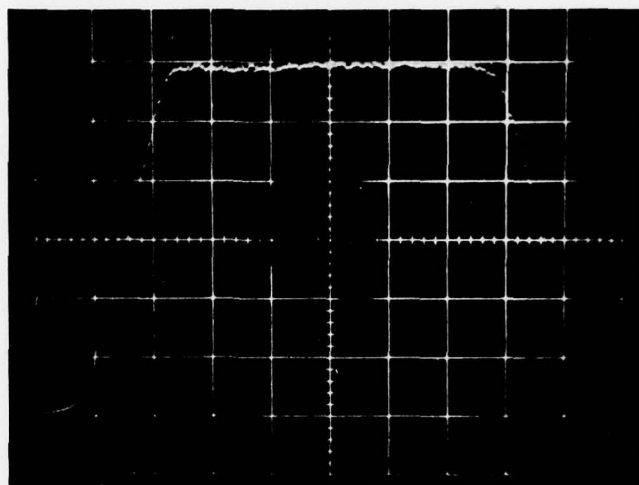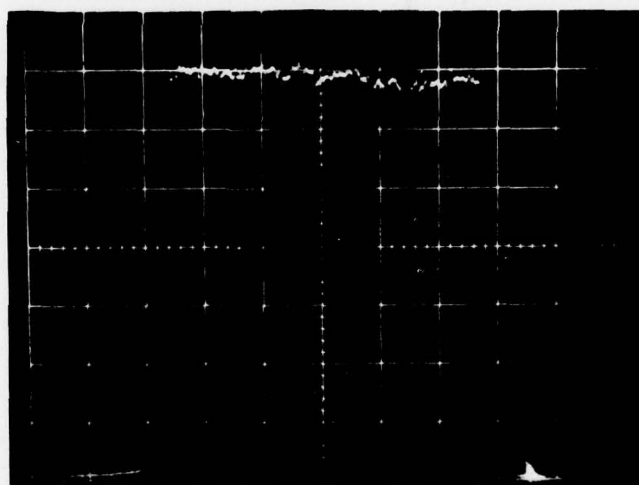Fig. 2-4 — Timing of orthogonal MTF (and PTF) outputs
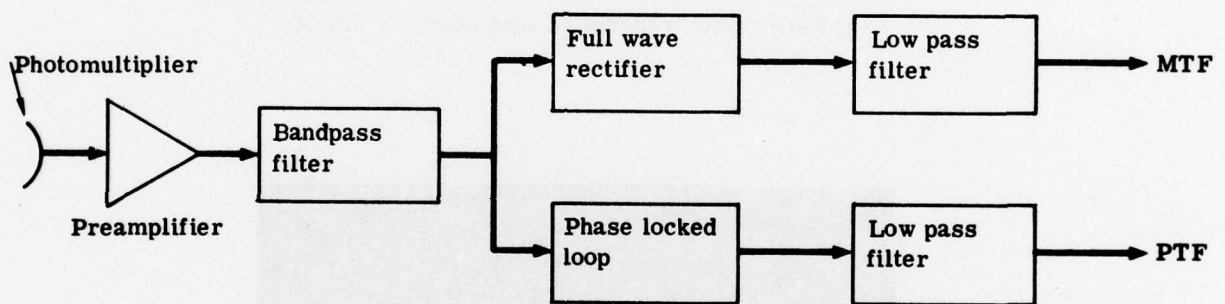
(a) Zero-order transmitted f/64 cone, λ = 0.6328

(b) First-order transmitted f/64 cone, λ = 0.6328

Fig. 2-5 — Transmitted zero-order and first-order beams for operational gratings

Fig. 2-6 — Basic electronic processing

the geometry of the diffracted beams. The angular velocity of the gratings = $2\pi/T$ radians per second.

From Fig. 2-7, it is apparent that the angular motion of each grating to cause the beams to go from zero overlap on one side to zero overlap on the other (giving the complete OTF) is β radians. From the diagram

$$\beta = a/r$$

also a = $D\alpha$

$$r = D\theta$$

therefore

$$\beta = \alpha/\theta$$

Hence the time, τ, for the OTF $= \dfrac{T}{2\pi} \cdot \beta$

$$= \frac{T}{2\pi} \cdot \frac{\alpha}{\theta}$$

Now $\theta = \lambda/s$, therefore $\tau = T\alpha s/2\pi\lambda$.

For the actual system T = 3.2×10^{-2} second, $\alpha = 1/64$, and S = 10^{-5} meter.

Using $\lambda = 5 \times 10^{-7}$ meter we obtain

$$t = 1.59 \times 10^{-3} \text{ second}$$

For $\lambda = 6.328 \times 10^{-7}$ meter

$$\tau = 2.014 \times 10^{-3} \text{ second}$$

2.5.1.2 Carrier Frequency

The frequency of the modulation caused by the interference of the beams from the two gratings may be calculated by consideration of Fig. 2-8, showing the two gratings at their parallel position (zero on the OTF curve).

The tangential velocity of each grating is v given by v = $2\pi L/T$ where L is the distance the optical axis of the system is separated from the rotational axis of the gratings.

The component of velocity in the direction perpendicular to the gratings (at an angle θ) is given by v cos θ. Hence the Doppler shifts of the diffracted beams are

$$\pm \frac{v \cos \theta}{s}$$

Hence the interference frequency

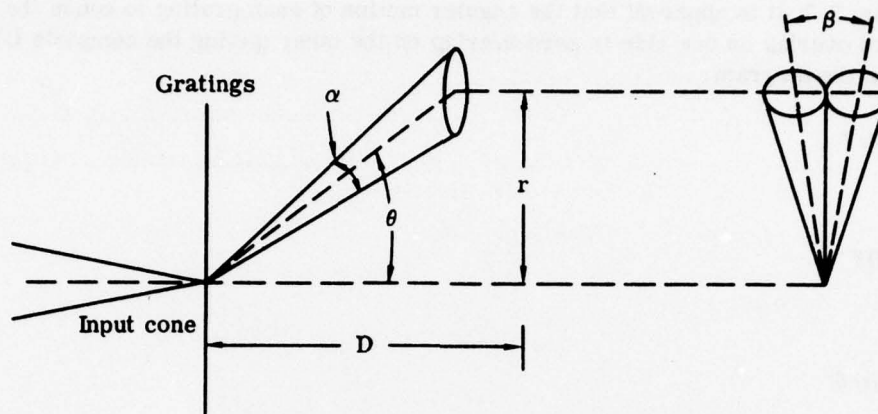$$\nu_0 = \frac{2v \cos \theta}{s} = \frac{4\pi L}{\sqrt{2} \; sT} \qquad (\theta = 45°)$$
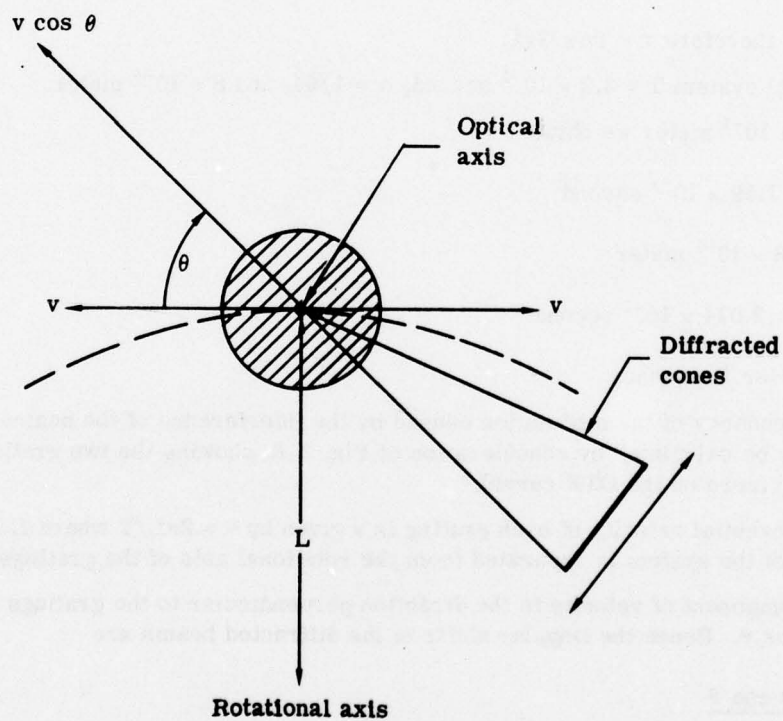
Fig. 2-7 — Geometry of diffracted beams

Fig. 2-8 — Two grating sections parallel

With L = 1.341 centimeters, S = 10^{-3} centimeters and T = 3.2×10^{-2} second

$$\nu_0 = 372 \times 10^3 \text{ Hz}$$

Because of the rotation of the grating, the frequency changes slightly during the course of the OTF. Corresponding to this change is a systematic phase change during the course of the OTF output. This phase variation may be found as follows (from consideration of Fig. 2-8).

From the full overlap position (grating lines parallel) one grating rotates an angle ψ in one direction and the other rotates ψ in the opposite direction.

The two Doppler frequency shifts then become

$$\nu_1 = v \cos (\theta + \psi)/s$$

$$\nu_2 = v \cos (\theta - \psi)/s$$

Modulation frequency

$$\nu = \nu_1 + \nu_2$$
$$= v \cos (\theta + \psi)/s + \cos (\theta - \psi)$$
$$= 2v (\cos \theta \cos \psi)/s$$
$$= 2v \cos \theta/s \ [1 - \psi^2/2]$$
$$= \nu_0 \ [1 - \psi^2/2]$$

Thus the PMT ac output I(t) has the form

$$I(t) = \cos [2\pi \nu_0 (1 - \psi^2/2) \ t]$$
$$= \cos [2\pi \nu_0 t - \pi \nu_0 \psi^2/2 \ t]$$
$$= \cos [2\pi \nu_0 t - \phi(t)]$$

where $\phi(t) = \pi \nu_0 \psi^2 t$ represents the systematic phase function.

Now $t = \psi T/2\pi$, where T is the rotation time. Therefore

$$\phi(\alpha) = \frac{\nu_0 \psi^3 T}{2}$$

At the limit of the OTF $\psi = \beta /2 = S\alpha/2\lambda$ where S is the grating spacing and α is the cone angle of the focused beam. Hence

$$\phi = \frac{\nu_0 S^3 \alpha^3 T}{16\lambda^3}$$

With $\nu_0 = 372 \times 10^3$ Hz, S = 10 micrometers, α = 1/64, λ = 0.6328 micrometers, and T = 32 milliseconds, then

$$\phi = 11.2 \text{ radians}$$

2.5.2 Signal-to-Noise Ratio

2.5.2.1 MTF

As shown above, the output of each photodetector during an OTF scan time may be written as

$$I(t) = I_0 \left\{ 1 + M(t) \cos \left[\omega t + \phi(t) \right] \right\}$$

where I_0 represents the current due to the total optical flux on the detector, $M(t)$ is the MTF and $\phi(t)$ is the PTF. The quantum noise limited signal-to-noise ratio will therefore be given by $S/N = M(I_0/2eB)^{1/2}$ where e is the charge as an electron, and B is the system bandwidth. To find the expected signal-to-noise ratio for a star source of particular visual magnitude requires knowledge of the source spectral distribution, telescope aperture, system transmission, and sensor spectral response. Now by definition* the illuminance of a 0 magnitude star (outside the atmosphere = 2.54×10^{-6} lumen/m^{-2}.

Also, luminous efficiency of the sun is 93.4 lumens per watt. Hence the irradiance H_0 of a 0 magnitude (sun-like) star is given by

$$H_0 = 2.54 \times 10^{-6}/93.4 = 2.72 \times 10^{-8} \text{ wm}^{-2}$$

A computer program (BLKBDY) is available for integration of spectral responses to black-body radiation. This can give the response of a photodetector in amperes for total input watts for unfiltered or atmospherically filtered radiation. This has been exercised for an RCA C20 photo-cathode† cut-off at 0.4 and 0.7 micrometer for a 5,900 °K blackbody. The resulting response, β, is given by

$$\beta = 16.1 \times 10^{-3} \text{ amp w}^{-1}$$

Hence for a zero magnitude star, I_0, the photocathode current is given by

$$I_0 = 2.72 \times 10^{-8} \times 16.1 \times 10^{-3} A_T T_A T_T T_S$$

where A_T = telescope area = 2.0 square meters
T_A = atmospheric transmission = 0.7
T_T = telescope transmission to RTAM = 0.5
T_S = RTAM transmission = 0.076 (based on measured optical transmission of 0.38 and average efficiency of gratings)

Hence $I_0 = 2.3 \times 10^{-11}$ ampere (0 magnitude star).

The equivalent value for a first magnitude star is

$$I_0 = 9.3 \times 10^{-12} \text{ ampere (first magnitude star)}$$

Using a system bandwidth of 3×10^4 Hz and the electronic charge of 1.6×10^{-19} coulomb, we then obtain the signal-to-noise ratio for the zero or origin of the MTF curve.

---

* Allen, C.W., "Astrophysical Quantities," 3rd ed., Athlone Press, 1972.
† "RCA Electro-Optics Handbook", Technical Series EOH-11, RCA Corporation, 1974.

$$S/N = \frac{9.3 \times 10^{-12}}{3.2 \times 10^{-19} \times 3 \times 10^4} = 31$$

This represents the expected signal-to-noise ratio for a first magnitude star for the MTF at zero spatial frequency (i.e., at the time of complete pupil overlap). The value of the short exposing MTF at higher spatial frequencies typically has values of 0.06 or less. The signal-to-noise ratio for the MTF curves in this range will therefore be less than 2:1.

2.5.2.2 MTF Pedestal

The basic processing electronics providing the MTF curves produces in situations of low signal-to-noise ratio a signal-dependent offset that appears on the MTF curves as a pedestal. The output from the photodetectors is processed to give the MTF as indicated in Fig. 2-6 by passing it first through a bandpass filter (relatively wide-band), followed by full-wave rectification, and low-pass filtering the result. It is clear that even with no signal modulation (zero MTF value) there will be quantum noise fluctuations on the output of the bandpass filter. Full wave rectification and low pass filtering of these fluctuations will result in an essentially DC pedestal for the MTF curve. The offset component is signal (or MTF) dependent however, as can be seen from the following considerations.

The average photocathode current I_0 provides a quantum-noise term at the output of the bandpass filter whose variance (σ^2) is given by

$$\sigma^2 = 2I_0 eB$$

where B is the bandwidth of the bandpass filter. This noise function, y(t) will have an approximate Gaussian probability distribution, P(y), given by

$$P(y) = \frac{1}{\sigma(2\pi)^{1/2}} \exp\left(-y^2/2\sigma^2\right)$$

After full wave rectification the function y(t) becomes y'(t) where all negative values of y are made positive. The distribution of y' will now be related to P(y) by

$$P(y') = 2P(y) \text{ for } y' \geq 0$$

Thus

$$P(y') = \frac{2 \exp\left(-y^2/2\sigma^2\right)}{\sigma(2\pi)^{1/2}}$$

The result of low pass filtering (or integration) of y'(t) will then be to produce an offset value O given by

$$O = \int_0^\infty y' \, P(y')dy'$$

$$= \frac{2}{\sigma(2\pi)^{1/2}} \int_0^\infty y' \exp\left(-y'^2/2\sigma^2\right) dy'$$

2-13

$$= - \frac{2}{\sigma(2\pi)^{1/2}} \left[\sigma^2 \exp(-y'^2/2\sigma^2) \right]_0^\infty$$

$$= \frac{2}{\pi} \sigma$$

$$= 2(I_0 eB/\pi)^{1/2}$$

Now consider the situation when the MTF is not zero but there is an instantaneous value of signal, S, (representing some position of the fluctuating carrier frequency between its limits of $I_0(1 \pm M)$. Now it is only those noise excursions y(t) that exceed S that are rectified and will be integrated to give the offset O(S). Thus we obtain (for S either positive or negative)

$$O(S) = \frac{2}{\sigma(2\pi)^{1/2}} \int_S^\infty y' \exp(-y'^2/2\sigma^2) \, dy'$$

$$= \frac{2\sigma^2 \exp(-S^2/2\sigma^2)}{\sigma(2\pi)^{1/2}}$$

$$= \sigma \left(\frac{2}{\pi} \right)^{1/2} \exp(-S^2/2\sigma^2)$$

Now the value S represents only an instantaneous value of the carrier frequency oscillation (sinusoidal) over the range $I_0(1 + M)$. To find the average value of the offset for a particular value of MTF, M requires that O(S) be weighted by the probability of S. Now we can write $S = M \sin \omega t$ where ω is the carrier frequency. Hence

$$P(S) = P(M \sin \omega t)$$

$$= \frac{2}{2\pi (M^2 - S^2)^{1/2}}$$

Therefore the average offset $\overline{O}$ is given by

$$\overline{O} = \int_{I_0(1-M)}^{I_0(1+M)} O(S) \, P(S) \, ds$$

$$= \int_{I_0(1-M)}^{I_0(1+M)} \sigma \left(\frac{2}{\pi} \right) \exp(-S^2/2\sigma^2) \frac{1}{\pi(M^2 - S^2)^{1/2}} \, ds$$

$$= \frac{\sigma}{\pi} \left(\frac{2}{\pi} \right)^{1/2} \int_{I_0(1-M)}^{I_0(1+M)} \frac{\exp(-S^2/2\sigma^2)}{(M^2 - S^2)^{1/2}} \, ds$$

This integral has not been explicitly evaluated. From considerations of how $\overline{O}$ depends on modulation, it is clear that $\overline{O}$ is a minimum for M = 1. Consequently to compare for a recorded MTF the measured signal-to-noise ratio to the expected signal-to-noise ratio, the total height of the MTF at zero frequency should be compared to the rms noise riding on the pedestal. Neglecting the

2-14

effects of photon fluctuations then, the full wave rectification of the sinusoidal signal $I_0 \sin \omega t$ will provide after integration or envelope detection of value P given by

$$P = \frac{2}{T} \int_0^{T/2} I_0 \sin \omega t \, dt$$

where $T = 2\pi/\omega$, therefore

$$P = \frac{\omega I_0}{\pi} \int_0^{\pi/\omega} \sin \omega t \, dt$$

$$= \frac{I_0}{\pi} \left[-\cos \omega t \right]_0^{\pi/\omega}$$

$$= \frac{2 I_0}{\pi}$$

Now the offset O for the $M = O$ was shown above to be given by

$$O = 2 \left(\frac{I_0 e B}{\pi} \right)^{1/2}$$

therefore

$$P/O = \frac{2 I_0}{\pi} \cdot \frac{1}{2} \left(\frac{\pi}{I_0 e B} \right)^{1/2}$$

$$= \left(\frac{I_0}{\pi e B} \right)^{1/2}$$

For a first magnitude star $I_0 = 9.3 \times 10^{-12}$ ampere, expected, B is the bandwidth of the bandpass filter and for the final system, $B = 2 \times 10^5$. Hence

$$P/O \simeq \left(\frac{9.3 \times 10^{-12}}{\pi \times 1.6 \times 10^{-19} \times 2 \times 10^5} \right)^{1/2}$$

$$\simeq 9.6$$

This is consistent with values actually obtained.

3. BENCH TESTS

Prior to initial installation and testing of the RTAM on the 61-inch telescope at AMOS, bench tests were carried out during July of 1976. These were primarily aimed at demonstrating correct MTF and PTF timing, and expected signal-to-noise ratio. Tests of signal-to-noise ratio were principally carried out using a helium-neon laser. Figs. 3-1 through 3-7 show the resulting MTF traces for various input power levels. Measurements of signal-to-noise ratios are made for the various MTF curves and the values compared to the expected theoretical values [based on the relationship $S/N = I/(2eB)^{1/2}$, where I is the expected photocathode current, e is the electric charge, and B is the system bandwidth]. The values clearly agree closely for the HeNe input over the range measured.

Signal-to-noise tests were also carried out using an unfiltered tungsten source focused on a pinhole, and collimated as input to the RTAM. These tests also gave S/N values close to the expected values. However, as was learned later, such a dominantly red source does not adequately simulate a typical star white light source and chromatic effects occurred within the system to decrease S/N with such sources.
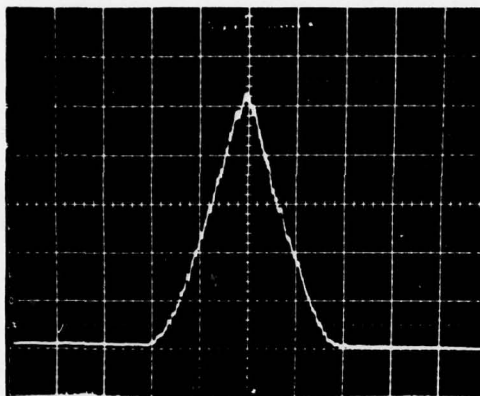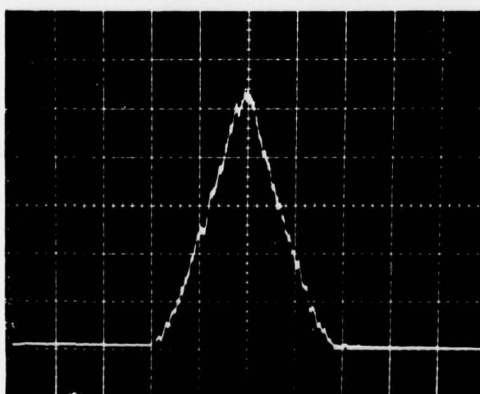
(a) Bandwidth   20 kHz
    Calculated S/N   473 : 1
    Actual S/N   167 : 1
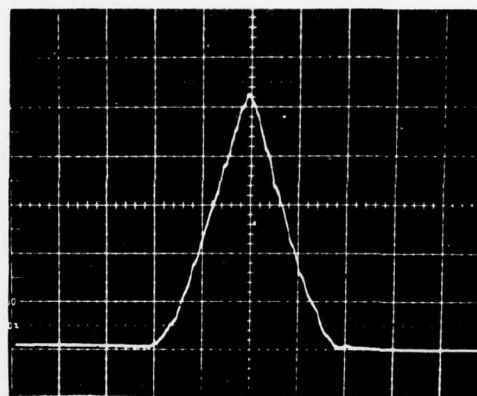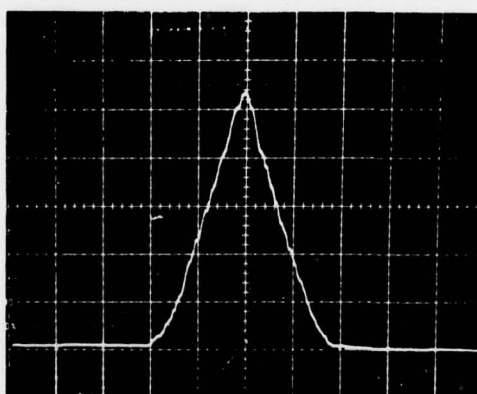
(b) Bandwidth   7.5 kHz
    Calculated S/N   772 : 1
    Actual S/N   >167 : 1

Fig. 3-1 — Input power 5.1×10^{-7} watt

(a) Bandwidth   20 kHz
    Calculated S/N   293 : 1
    Actual S/N   130 : 1

(b) Bandwidth   7.5 kHz
    Calculated S/N   478 : 1
    Actual S/N   >130 : 1

Fig. 3-2 — Input power 1.92×10^{-7} watt
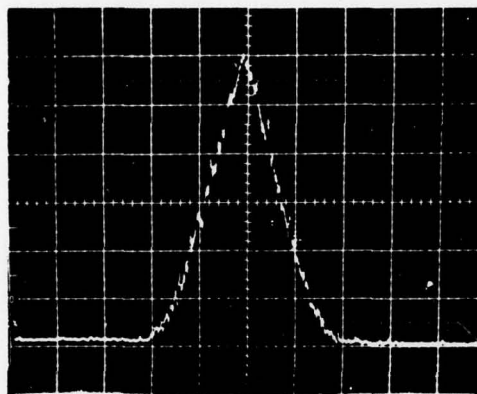
(a) Bandwidth   20 kHz
    Calculated S/N   155 : 1
    Actual S/N   100 : 1

(b) Bandwidth   7.5 kHz
    Calculated S/N   253 : 1
    Actual S/N   >100 : 1

Fig. 3-3 — Input power 5.5×10^{-8} watt

(a) Bandwidth   20 kHz
    Calculated S/N   98 : 1
    Actual S/N   65 : 1

(b) Bandwidth   7.5 kHz
    Calculated S/N   160 : 1
    Actual S/N   >65 : 1

Fig. 3-4 — Input power 2.2×10^{-8} watt

<table>
<tr><td>(a)</td><td>Bandwidth</td><td>20 kHz</td></tr>
<tr><td></td><td>Calculated S/N</td><td>61 : 1</td></tr>
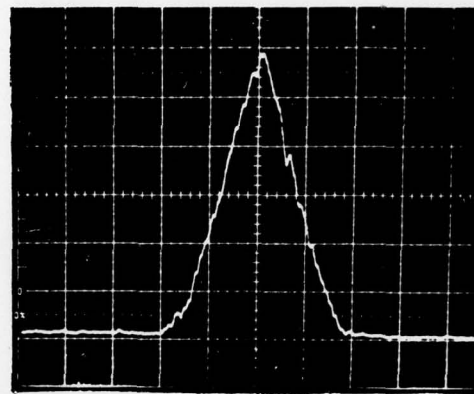<tr><td></td><td>Actual S/N</td><td>52 : 1</td></tr>
</table>

<table>
<tr><td>(b)</td><td>Bandwidth</td><td>7.5 kHz</td></tr>
<tr><td></td><td>Calculated S/N</td><td>99 : 1</td></tr>
<tr><td></td><td>Actual S/N</td><td>> 52 : 1</td></tr>
</table>

Fig. 3-5 — Input power 2.3×10^{-9} watt

<table>
<tr><td>(a)</td><td>Bandwidth</td><td>20 kHz</td></tr>
<tr><td></td><td>Calculated S/N</td><td>32 : 1</td></tr>
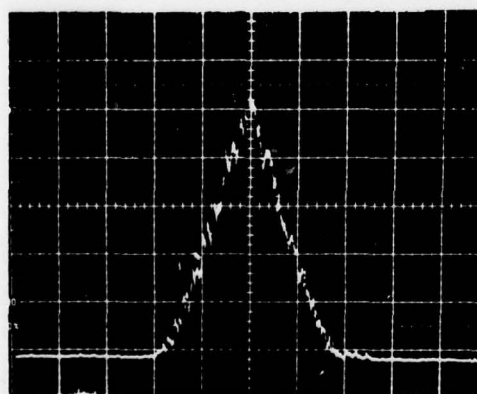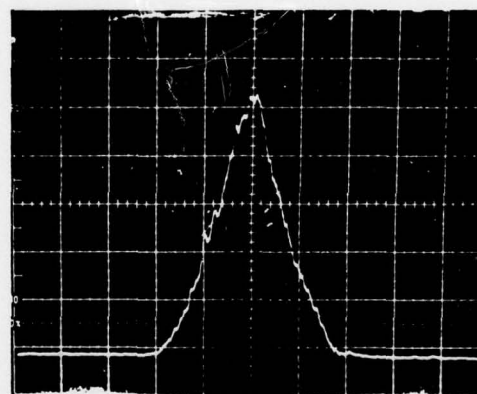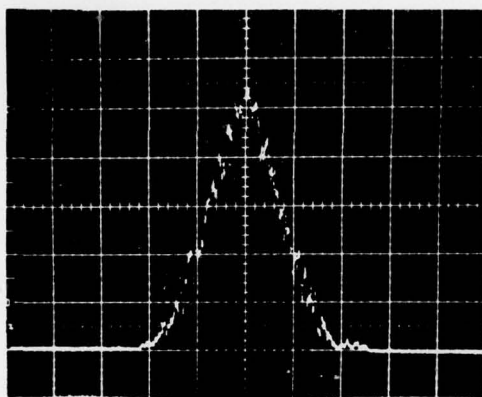<tr><td></td><td>Actual S/N</td><td>28 : 1</td></tr>
</table>

<table>
<tr><td>(b)</td><td>Bandwidth</td><td>7.5 kHz</td></tr>
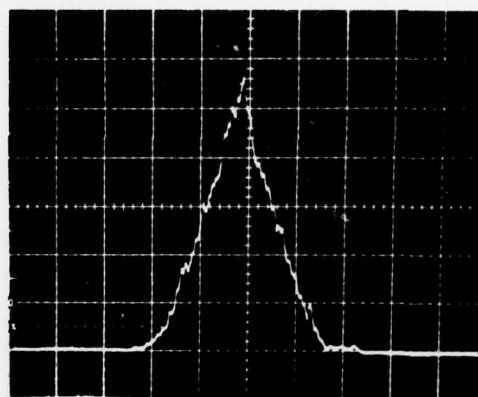<tr><td></td><td>Calculated S/N</td><td>52 : 1</td></tr>
<tr><td></td><td>Actual S/N</td><td>47 : 1</td></tr>
</table>

Fig. 3-6 — Input power 2.3×10^{-9} watt

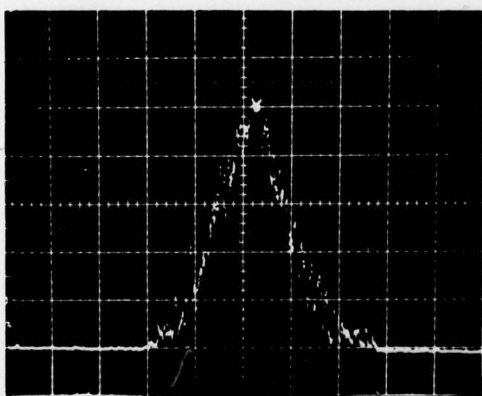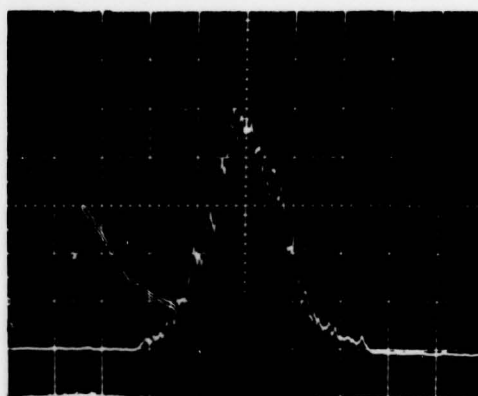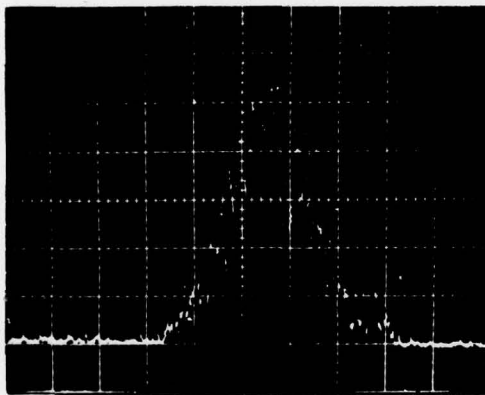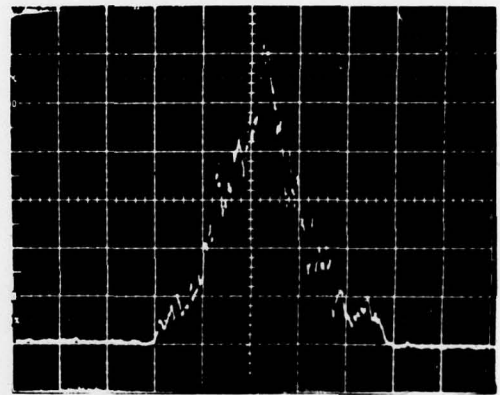(a) Bandwidth   20 kHz
    Calculated S/N   22 : 1
    Actual S/N   21 : 1

(b) Bandwidth   7.5 kHz
    Calculated S/N   36 : 1
    Actual S/N   30 : 1

Fig. 3-7 — Input power 1.1×10^{-9} watt

4. INITIAL INSTALLATION AT AMOS

The RTAM was packed and shipped to Maui for installation and test during the two-week period of August 21 to September 3, 1976. After initial bench tests established the same baseline performance achieved at Itek, the system was mounted and aligned on the atmospheric seeing package (ASP) on the 1.6-meter telescope during the night of August 24, 1976. MTF recordings made over subsequent nights' operations using bright stars as inputs brought to light three particular shortcomings of the RTAM as configured at that time:

1. Significantly lower signal-to-noise ratios were observed on MTF outputs than expected (factor of 2 to 3).

2. The PTF outputs became random when the MTF value drops to zero.

3. The system field of view was very small, producing large variations of MTF output with small telescope misalignment.

Examination of the modulation on the output of a photodetector showed it to be typically about 35 percent for a star input (Vega). This loss in modulation (which becomes a direct loss in signal-to-noise ratio) was attributed to chromatic aberrations in the lenses imaging one grating onto the other. An attempt was made using substitute lenses (loaned by Avco Corporation) between the gratings to increase the modulation and therefore the signal-to-noise ratio. This was partially successful, particularly on a single channel yielding a modulation of appoximately 80 percent and a signal-to-noise ratio at the MTF zero spatial frequency on Vega near the expected value (30:1). However, the introduction of the substitute lenses was found to reduce the system field of view to an unacceptable value (approximately 1 arc-second). This field of view reduction occurred because of vignetting effects caused by the shorter focal length of the substitute lenses. It was determined that to solve the field of view and chromatic problems simultaneously, a careful redesign of the optical train between the two gratings was required.

The phase transfer function was obtained by using a phase locked loop to detect the change of frequency as a function of time, and integrating this change to give an instantaneous phase value. This method is perfectly adequate provided the MTF signal-to-noise ratio remains above some threshold. When the signal-to-noise ratio drops below this value (for long enough) the phase lock loop goes out of lock and random phase values are recorded thereafter. Because the MTF for a real atmosphere drops to zero throughout the spatial frequency spectrum, giving a zero signal-to-noise ratio at those points, this random phase output was found to occur. Analysis of the phase locked loop parameters indicated that for a signal-to-noise ratio at more than 2 the loop would go out of lock.

Oscilloscope recordings of MTF's and PTF's taken during the preliminary installation period have been included in the Avco report.*

---

*Miller, M.G., and Zieski, P.L. Turbulence Environment Characterization, Interim Technical Report, Contract F30602-76-0054 (Avco Everett Research Laboratory) RADC Technical Report RADC-TR-77-70 (Mar 1977), A038632.

5. MODIFICATIONS TO RTAM

Subsequent to the initial tests at AMOS, the RTAM was returned to Itek and some optical and electronic modifications were made to the equipment. The principal limitation on operational performance was found to be a restricted field of view and lack of achromatism. In addition, it was felt that the phase output of the system would not give satisfactory or dependable results for low signal-to-noise ratios, or after the MTF drops to zero. The following describes the modifications that were introduced in an effort to overcome these deficiencies.
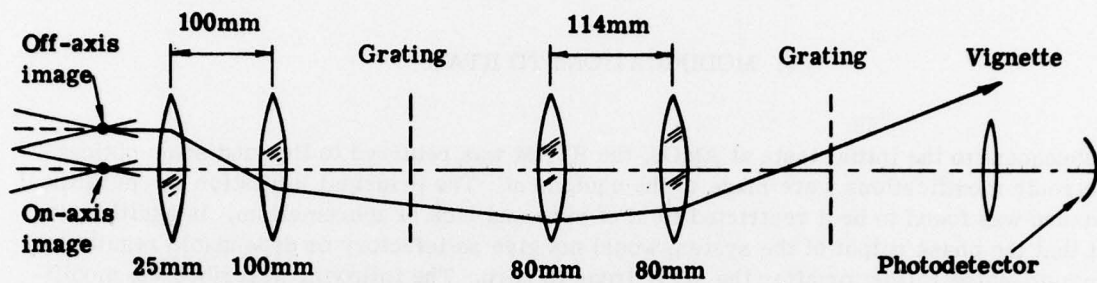
5.1 OPTICAL

The optical train from the star image position to one of the detectors for the original system is shown schematically in Fig. 5-1. (The mirrors are excluded for clarity). The solid line shows the principal ray of the cone for the on-axis image (only the zero-order between the gratings is shown, the first-order rays run parallel to, but displaced from, the zero-order rays, between the two lenses between the gratings). The dotted line shows the principal ray for the star image on an off-axis position. Because of the lack of telecentricity between the lens combinations L1 and L2, L3 and L4, it is clear that for an off-axis image position the rays rapidly deviate from the optical axis in the neighborhood of lens L4 and more particularly in the neighborhood of lens L5, which gathers the interfering orders onto a photodetector. Vignetting occurred at these positions. Which lens was the limiting aperture depended to some extent on which MTF slice was involved, and the direction of the off-axis movement. The substitute lenses, L3 and L4, gave superior chromatic performance but the vignetting effect became even more serious since these lenses had a focal length of 60 millimeters as opposed to the original 80 millimeters. The vignetting effects were reduced and the field of view was extended by using alternate lenses with modified separations to provide the telecentric arrangement shown in Fig. 5-1b. With this arrangement the rays never stray very far from the optical axis. In addition, the alternate lenses chosen for L3 and L4, which provide the imaging between the gratings were also selected for minimum chromatic aberration. To ease optical alignment of the system, the mounting arrangements for the lenses and the K-mirrors between the gratings were also modified.

Another optical modification made was in the region between the second grating and the photomultipliers. In the original system the X and Y diffracted beams were directed to alternate detectors by means of two mirrors. This arrangement also introduced vignetting in off-axis field positions therefore it was decided to image both X and Y beams onto a single detector and electronically switch between the two channels as will be described.
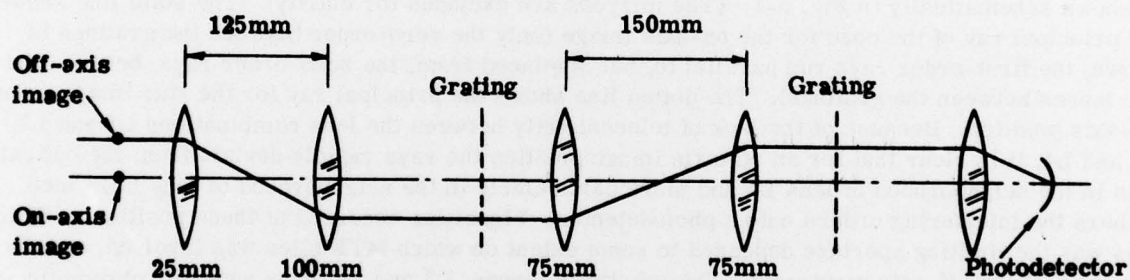
5.2 ELECTRONIC MODIFICATIONS

A number of circuit changes have taken place in the RTAM system since the publication of the RTAM Operation and Maintenance Manual dated July 1975. These changes are as follows:

(a) Original system (non-telecentric)

(b) Final system (telecentric)

Fig. 5-1 — Original and final optical layouts of RTAM

1. One photomultiplier tube (PMT) detector is employed to detect both the X and the Y optical transfer function (OTF) instead of a separate PMT detector for X and Y OTF's. There are two primary reasons for employing one common PMT detector for detecting both X and Y OTF's. The first is that the optical design for directing/centering the X and Y first-orders from the second grating onto a single PMT photocathode is easier. The second is that any gain and sensitivity differences between two separate PMT detectors is eliminated by using a single PMT detector.

2. The phase detector used for obtaining the phase transfer function was completely redesigned. The reason for this redesign was to prevent the loss of the PTF information under certain conditions. If, during the OTF measurement the MTF went to zero, the phase information would also be lost (as would be expected) however, the phase information became indeterminate from that point on regardless of what the MTF response did. The new phase detector is designed to recover its phase information when the MTF recovered.

3. The timing that is derived from the outer periphery of the second grating was changed to accommodate the use of a single PMT detector to detect both the X and Y OTF's. The implication is that the signal processing channel has to be demultiplexed in order to separate and identify X information from Y information.

4. Demultiplexing circuitry was added in order to direct X and Y MTF/PTF data to their respective coaxial driver/lines.

5. The automatic gain control (AGC) of the PMT was defeated and a manual PMT gain control potentiometer was mounted on the control console front panel. The reason for this change is that the optimum gain of the PMT is better controlled manually for an optimum signal-to-noise ratio.

RTAM Signal Processing Diagram (Fig. 5-2)

The PMT detects both X and Y OTF information that is amplified by the video amplifier. As can be seen, the operator can vary the PMT gain via the potentiometer located on the control console. Care should be taken not to increase the PMT gain to a point where the MTF/PTF information is saturated, thus giving less than optimum results. This can be guarded against by viewing the MTF/PTF available at the control console via an oscilloscope. The video amplifier output signal is further amplified selectively by the bandpass filter, whose center frequency is centered around the grating frequency of 370kHz. The bandpass filter output signal is then sent to both the MTF and PTF electronics. The MTF electronics has not been changed and is described in the RTAM Operation and Maintenance Manual. The only portion that is different is the addition of an MTF/PTF demultiplexer (see Fig. 5-3). A dual demultiplexer is used, the first part is used for demultiplexing X and Y MTF data, whereas the second part of the demultiplexer is used for selecting either X or Y PTF data. The selection of X or Y data is determined by the code received on the A_0/A_1 control lead. A low signal (0 volts) selects X MTF and X PTF, whereas a high signal (+5 volts) selects Y MTF and Y PTF. The output signals of the demultiplexers are buffered and sent to their respective coaxial drivers. The coaxial driver functions are specified in the RTAM Operation and Maintenance Manual.

The PTF electronics, or phase detector, has been changed and is shown in detail in Fig. 5-4. The two signals to be compared are the detected signals during X or Y MTF and the preset signal of the voltage controlled oscillator (VCO). The latter signal frequency can be changed by the operator at the control console. The proper phase detection requirement for these two signals is that their frequencies be identical.

The function of comparators A_1 and A_2 is to convert low level signals to logic level signals. The phase detector shown in Fig. 5-4 is a ±180-degree phase detector. The D inputs of each of these edge-triggered flip-flops are hard wired to +5 volts. The clocks inputs, T serve as the

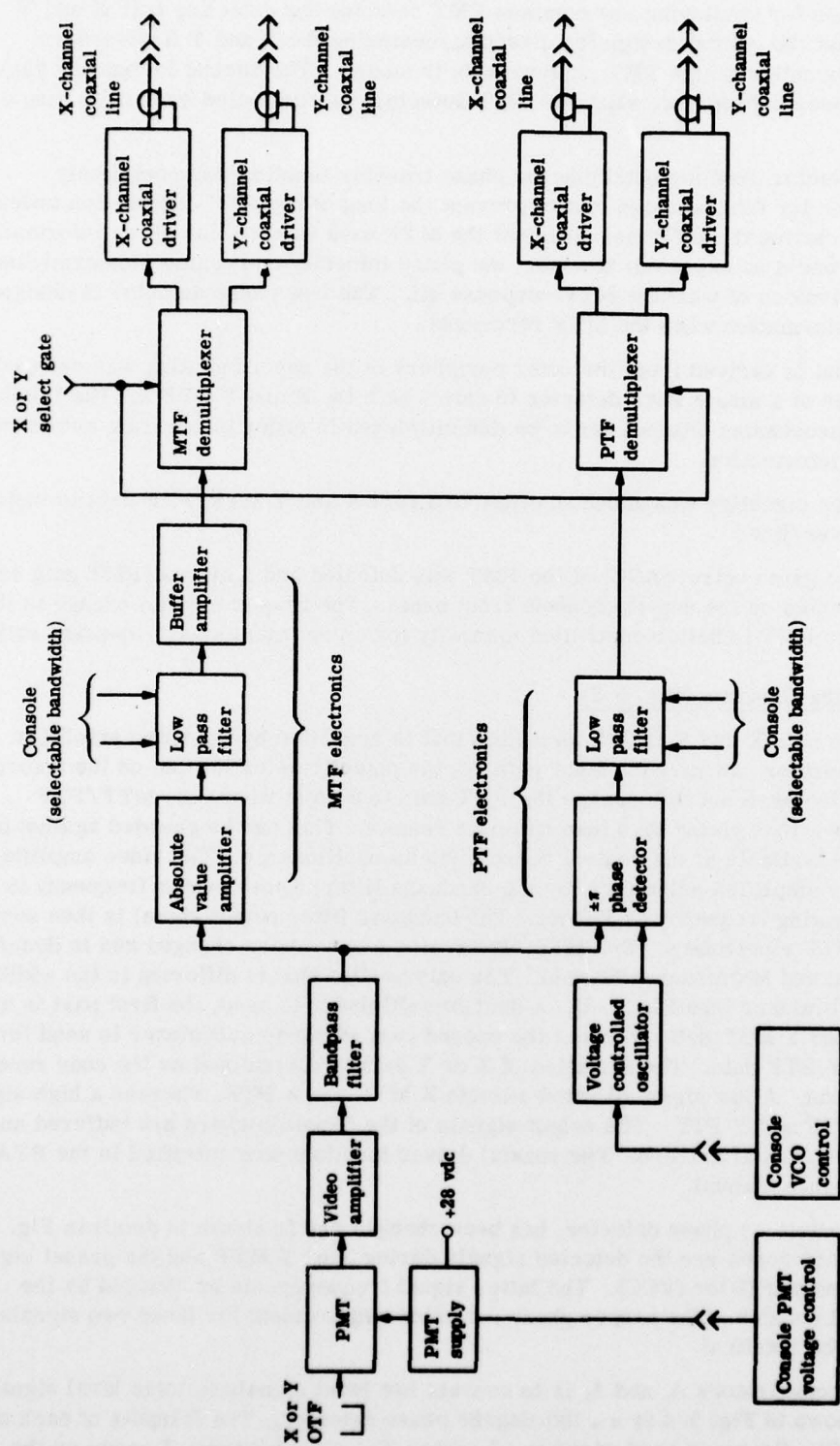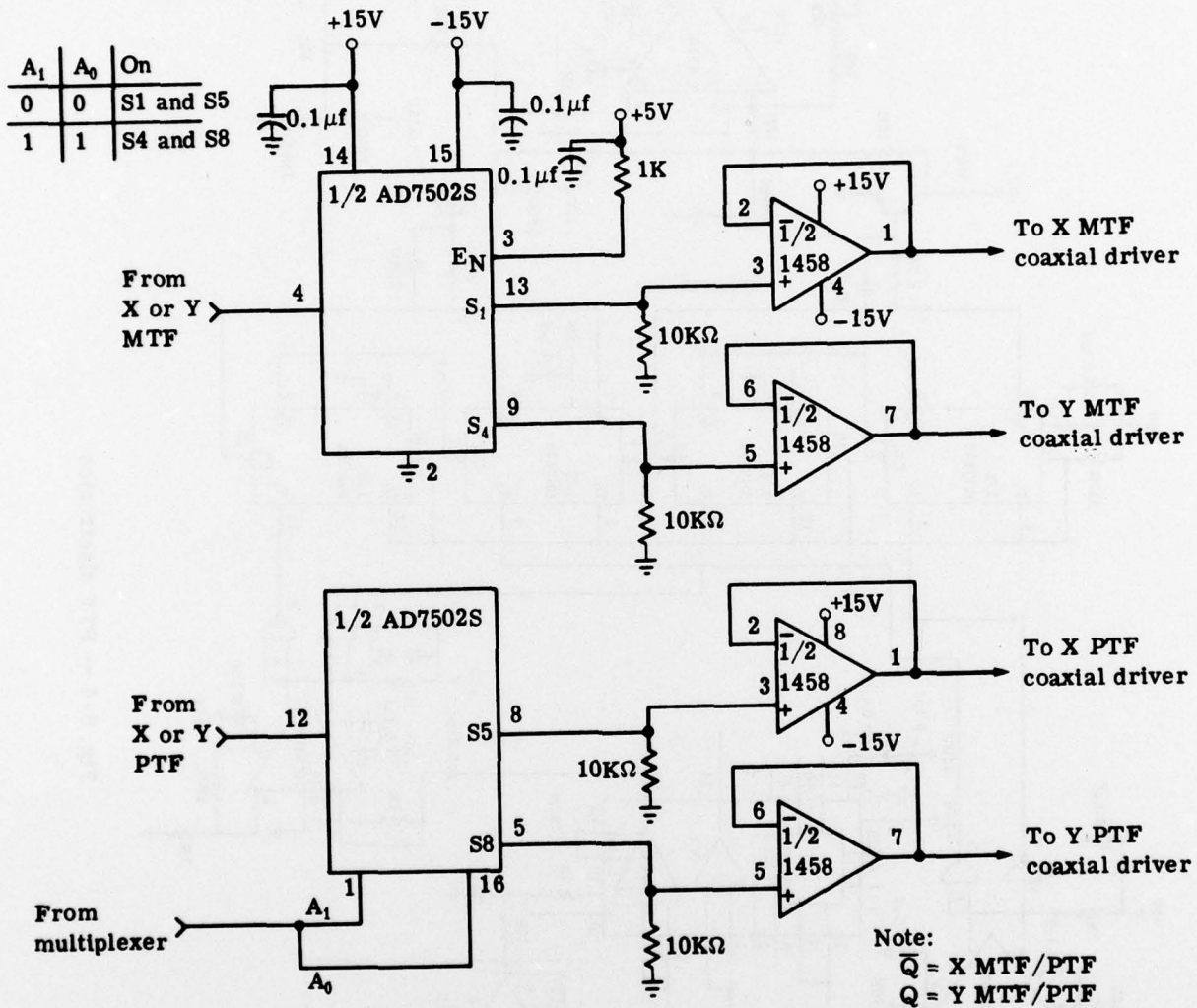Fig. 5-2 — RTAM signal processing electronics

A_1	A_0	On
0	0	S1 and S5
1	1	S4 and S8

Fig. 5-3 — MTF/PTF demultiplexer

Note:
$\overline{Q}$ = X MTF/PTF
Q = Y MTF/PTF

Fig. 5-4 — PTF electronics

inputs to these flop-flops or edge-triggered phase detector, where the information (+ 5 volts) at the D inputs appears at the Q output of each flip-flop for each positive clock transition at the T inputs.

The positive transition of A_{1-7} output signal transfers the D input's hard-wired 1 to the Q_1 output, which causes Q_1 to go high and removes the inhibit from CL_2. Q_2 is high during this period and remains high until a positive transition is received from comparator A_{2-7}, at which time Q_1 is reset to 0. The width of the pulse at Q_1 is directly proportional to the phase difference between the detected signal frequency and the VCO frequency. This pulse is integrated by Q_1 and op-amp A_3 to produce an output voltage that is proportional to the pulse width of the phase detected signal. The lower two flip-flops work exactly the same as the top two, but for the second half of the period of the measured signal. The offset adjust located at the bottom right of Fig. 5-4 is adjusted such that the op-amp output is exactly 0V for the condition of zero phase difference between the two signal frequencies. The gain of the op-amp is then adjusted for −10V and + 10V for + 180-degree phase and −180-degree phase shift respectively. The output of the phase detector then is inputted into a selectable low-pass filter as explained in the RTAM Operation and Maintenance Manual. The PTF demultiplexer works in the same manner as explained for the X or Y MTF units, where the X and Y PTF information is sent to its proper coaxial line driver.

The system timing generator (Fig. 5-5) determines when the demultiplexer outputs X or Y data. As described in the RTAM Operation and Maintenance Manual, the system timing consists of detecting when X gratings (or Y gratings) are about to overlap each other. This is done by opaquing the periphery of the second rorating grating at each X subaperture, therefore, the LED-detector pair is energized and produces a positive going pulse to pin 1 of the comparators (shown in Fig. 5-5) each time the X shear has increased to 100 percent shear (minimum MTF) from a 0 percent shear (maximum MTF) condition. At this trailing edge of each X MTF response, the comparator is pulsed and starts the delay monostable multivibrator, the trailing edge of the delay monostable starts a 4-millisecond monostable. The purpose of the delay monostable is to delay the start of the 4-millisecond monostable such that the 4-millisecond gate is centered about the X MTF period. On the rotating glass substrate there are a total of 8 gratings (4 X and 4 Y) equally spaced around the glass substrate. The rotation rate of the glass substrate is 31.25 revolutions per second or 32 milliseconds per revolution, hence 4 milliseconds is alloted for each X or Y MTF/PTF. The 4-millisecond gate is inverted by the NAND gate shown in Fig. 5-4 and is the code for demultiplexing X MTF/PTF data. In the following 4-millisecond period the NAND gate output is high (+ 5 volts), this is the code for demultiplexing Y MTF/PTF data.
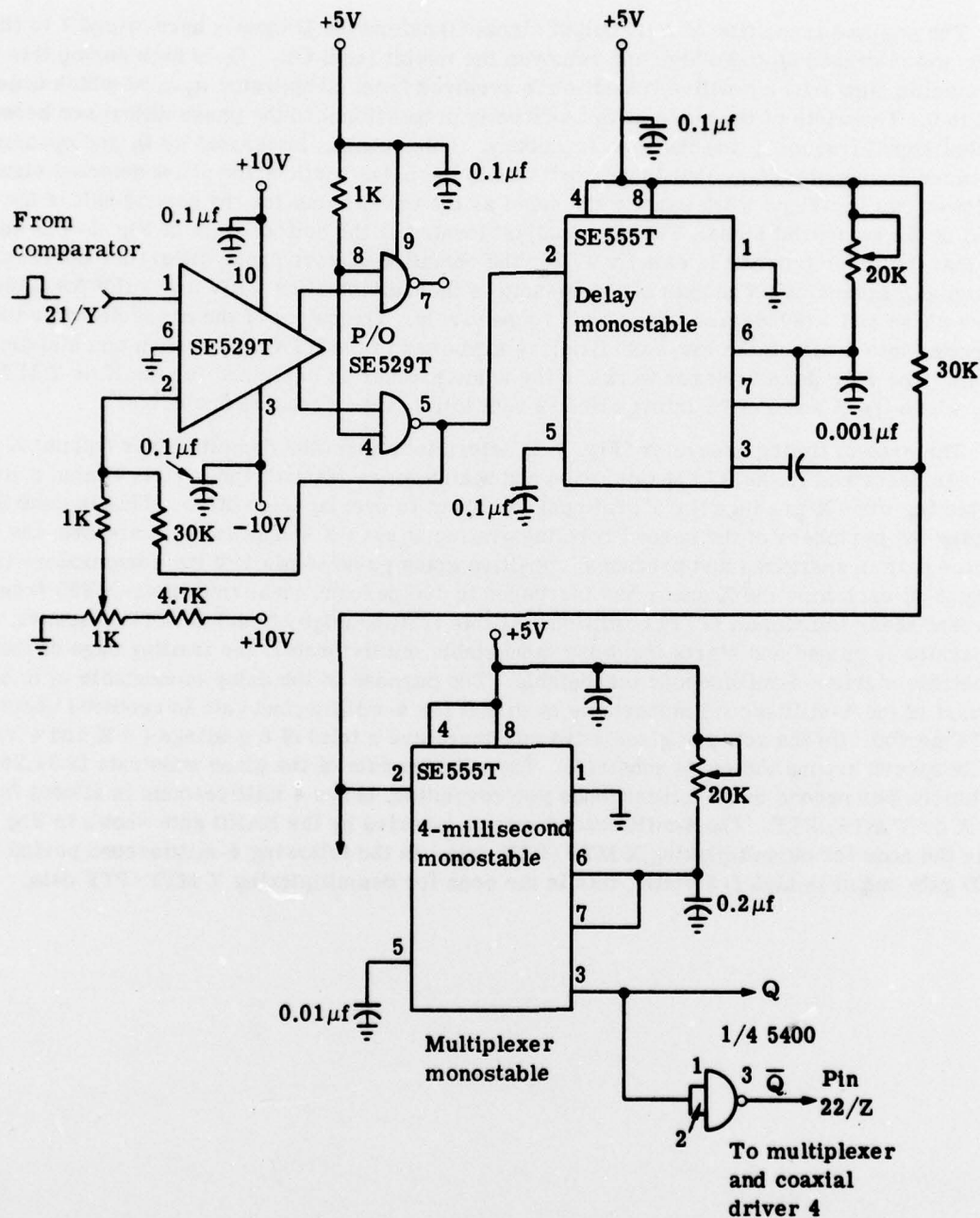
Fig. 5-5 — Timing generator

6. FINAL INSTALLATION AT AMOS

On completion of the optical and electronic modifications described above, the RTAM was reshipped to Maui for installation tests during the period of 24 to 28 January 1977. The detailed results of these tests together with photographic records of RTAM outputs are documented.*

The modifications that had been made to the system were designed principally to improve signal-to-noise for white light sources, and to increase field of view. As a result of the tests it was determined that provided the system is optimized for single channel operation, a signal-to-noise ratio close to the expected value is obtained for the zero of the MTF. For example, ratio of signal to rms noise of >20:1 is observed for the MTF's on page 65 of the above-mentioned reference. The expected value for first magnitude star is 30:1. The optimized measured photomultiplier signal modulation for a single channel was greater than 85 percent. The signal-to-noise ratio reduced significantly (signal modulation less than 60 percent) when both channels were equalized. Initially it had been thought that chromatic aberration was responsible for this modulation loss, and this assumption led to the introduction of lenses of superior chromatic performance. It was discovered in the course of the tests, however, that the cause of reduced system performance with broadband sources was due to residual spherical aberration in the lenses rather than to chromatic aberrations. The spherical aberration results in the optical path through the lenses being different for different wavelengths diffracted by the gratings. This in turn gives reduced modulation in the detector output as the ac signals for the different wavelengths vary in phase. The effect of the residual spherical aberration could be minimized for one channel at a time by arranging the optics so that the first-order and zero-order beams passed symmetrically through the imaging lenses (between the gratings) with respect to the optical axis. This could not be accomplished simultaneously for both X and Y OTF slices due to the geometry of the diffracted beams.

The modifications to the optical train did improve the field of view of the system to approximately ±4 arc-seconds for single channel operation.

---

*Miller, M.G., et al., Turbulence Environment Characterization, Interim Technical Report, Contract F30602-76-C-0054 (Avco Everett Research Laboratory), RADC Technical Report, RADC-TR-77-232, (July 1977).